View metadata, citation and similar papers at core.ac.uk
brought to you by CORE
provided by CERN Document Server

EUROPEAN ORGANIZATION FOR NUCLEAR RESEARCH
CERN — SL DIVISION

CERN SL-2002-043 (ECT)

Radioprotection Calculations for the TRADE Experiment

L.Zanini, A. Ferrari, A. Herrera-Martínez, Y. Kadi
CERN, Switzerland

C. Rubbia, N. Burgio, M. Carta, A. Santagata
ENEA, Italy

L. Cinotti
Ansaldo Nucleare, Italy

Abstract

The TRADE project is based on the coupling of, in a sub-critical configuration, of a 115 MeV, 2 mA proton cyclotron with a TRIGA research reactor at the ENEA Casaccia centre (Rome). Detailed radioprotection calculations using the FLUKA and EA-MC Monte Carlo codes were performed during the feasibility study. The study concentrated on dose rates due to beam losses in normal operating conditions and in the calculation of activation in the most sensitive components of the experiment.

Results show that a shielding of 1.4 m of barytes concrete around the beam line will be sufficient to maintain the effective doses below the level of 10 Mu Sv/h, provided that the beam losses are at the level of 10 nA/m.

The activation level around the beam line and in the water will be negligable, while the spallation target will reach an activation level comparable to the one of a fuel element at maximum burnup.

Presented at the Third International Workshop on the Utilisation and Reliability of High Power Proton Accelerators
Santa Fe
May 12-16 2002

Geneva, Switzerland
May 2002

RADIOPROTECTION CALCULATIONS FOR THE TRADE EXPERIMENT

L. Zanini*, A. Ferrari, A. Herrera-Martínez, Y. Kadi
CERN, CH-1211 Geneva 23, Switzerland

C. Rubbia, N. Burgio, M. Carta, A. Santagata
ENEA, 00196 Roma, Italy

L. Cinotti
Ansaldo Nucleare, 16161 Genova, Italy

for the TRADE collaboration†

Abstract

The TRADE project is based on the coupling, in a sub-critical configuration, of a 115 MeV, 2 mA proton cyclotron with a TRIGA research reactor at the ENEA Casaccia Centre (Rome). Detailed radioprotection calculations using the FLUKA and EA-MC Monte Carlo codes were performed during the feasibility study. The study concentrated on dose rates due to beam losses in normal operating conditions and in the calculation of activation in the most sensitive components of the experiment.

Results show that a shielding of 1.4 m of barytes concrete around the beam line will be sufficient to maintain the effective doses below the level of 10 μSv/h, provided that the beam losses are at the level of 1 nA/m.

The activation level around the beam line and in the water will be negligible, while the spallation target will reach an activation level comparable to the one of a fuel element at maximum burnup.

---

*Luca.Zanini@cern.ch

†The working group on TRADE: TRiga Accelerator Driven Experiment (ENEA, CEA, Ansaldo): TRADE Final Feasibility Report, Rome, March 2002

1 THE TRADE EXPERIMENT

The European Roadmap towards the experimental demonstration of ADS indicates a number of experiments that should allow testing the different components of such a system [1]. Dedicated experiments are included in the Roadmap for the study of the accelerator (IPHI, TRASCO), the target (MEGAPIE), the sub-critical core (FEAT, TARC, MUSE). In this framework, an experiment providing the first coupling between an accelerator and a sub-critical reactor is very useful from both licensing and experimental point of views. In fact, such an experiment will demonstrate the operation of an ADS system, from start-up to nominal power level, to shutdown, and will allow studying the relation between proton current and reactor power, the neutron source importance and reactivity effects.

C. Rubbia suggested to carry out this pilot experiment at the ENEA-Casaccia site where a 1 MW TRIGA research reactor is operating [2]. A cyclotron accelerating protons to 115 MeV, with a maximum current of 2 mA, will be built on the side of the reactor building. The reactor core will be modified, by replacing the central fuel rod with a spallation target of tungsten and by removing some other fuel rods (in particular the inner ring). The proton beam will be sent through a beam transport line to the reactor core, and will produce neutrons by spallation in tungsten.

Such an experiment presents additional radioprotection problems with respect

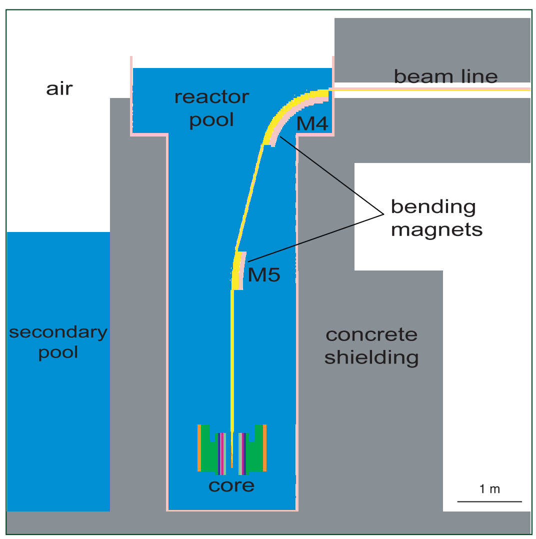

Figure 1: View of the geometry of the TRADE experiment as implemented in the FLUKA calculations.

to a normal reactor, because of the presence of the proton beam. In particular, one has to consider the following radioprotection issues: *i)* interaction of the proton beam with the target; *ii)* beam losses along the beam transport line in normal operating conditions; *iii)* radiation release in accident cases different from those of a conventional reactor.

In the following section we treat these cases concentrating in particular in the the first two topics. The third point has been treated extensively in Ref. [3].

2 SIMULATIONS

Monte Carlo simulations were performed using the FLUKA [4] and EA-MC [5] codes. In order to study the beam-target interaction and the radiation relase in accident cases, a full model of the TRIGA reactor including the additional features of the TRADE experiment was implemented. The geometry used in the simulations is shown in Fig. 1. Two bending magnets, labelled M4 and M5, which deviate the proton beam to the reactor core, were included. Before the M4 magnet a straight section of the beam line approximately 10 m long is foreseen to transport the beam from the accelerator to the reactor building. The same geometry was implemented in EA-MC in order to study by means of burnup calculations the activation of the target, of the water and of the air.

The problem of the radiation due to beam losses in normal conditions was treated differently. In this case, we followed two calculational schemes, one based entirely on FLUKA and a coupled FLUKA-EA-MC. In both schemes 110 MeV protons were generated, distributed along the length of the beam tube and propagated outwards. The calculations were done for 10^6 protons and scaled to 1 mA current.

2.1 Beam-target interactions

The distribution of neutrons generated in the spallation target unit and surrounding core structures is given in Fig. 2. Spallation neutrons are produced in a region extending radially up to 5 cm from the center of the core, that is a few cm before reaching the fuel elements. The neutron spectra from spallation and fission are different, and in the spallation more high-energy neutrons are produced; their average kinetic energy is of the order of 3-4 MeV. These neutrons are rapidly slowed down by the water moderator before reaching the core internal structures, therefore they do not represent a major problem in terms of radiation damage. We note that a few thermal neutrons, up to 10^9 n/cm^2/s/mA, will stream along the beam tube and slightly irradiate (1.3×10^{-5} Gy/s/mA) the lower permanent magnet, situated approximately 3 m above the core. On the other hand, the neutron leakage through the top of the reactor pool is negligible. We conclude that the shielding already present around the TRIGA reactor is sufficient to shield against the neutrons due

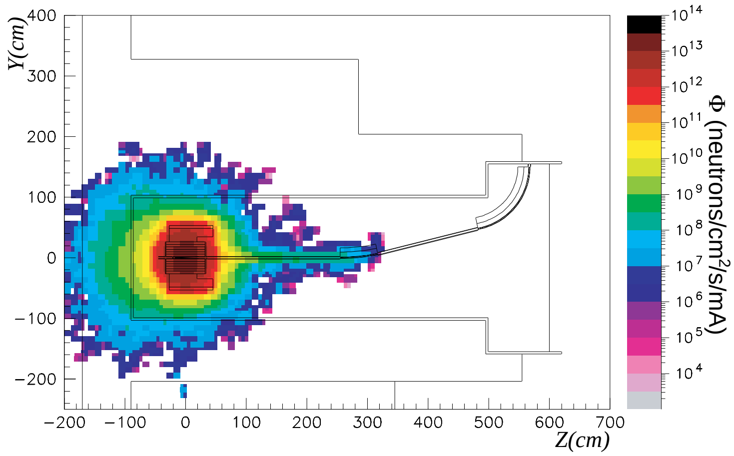

Figure 2: Neutron flux distribution ($n/cm^2/s/mA$) following the impact of the proton beam on a solid tungsten target in the TRADE experiment.

to beam-target interactions.

Concerning γ radiation, the photon flux reaching the top of the reactor pool is higher than the neutron flux, up to 10^4 $\gamma/cm^2/s/mA$. However, this flux does not constitute a problem in terms of effective dose. In Ref. [3] the results concerning this case are reported in more detail.

2.2 Radiation due to beam losses during normal operation

The most delicate aspect of the TRADE experiment is the coupling between the accelerator beam line and the reactor core. The beam is transported from the cyclotron to the reactor building through a shielded beam line. It is important to ensure that during the experiment the radiation released outside of the beam line does not exceed the allowable limits of exposure. This radiation originates from beam losses due to protons escaping from the beam line in normal operating conditions, and generating spallation neutrons in the beam tube and in the shielding. Typically, in the straight section of the beam line, the beam losses are expected to be of the order of 10^{-6}/m of the beam current. This will be the case for the portion of the beam line, approximately 10 m long, going from the accelerator to the reactor. On the other hand, when the beam is bent, like in correspondence to the M4 magnet (see Fig. 1), the losses are expected to be higher, of the order of 10^{-4}/m. Thus, the shielding will have to be carefully designed around the bending

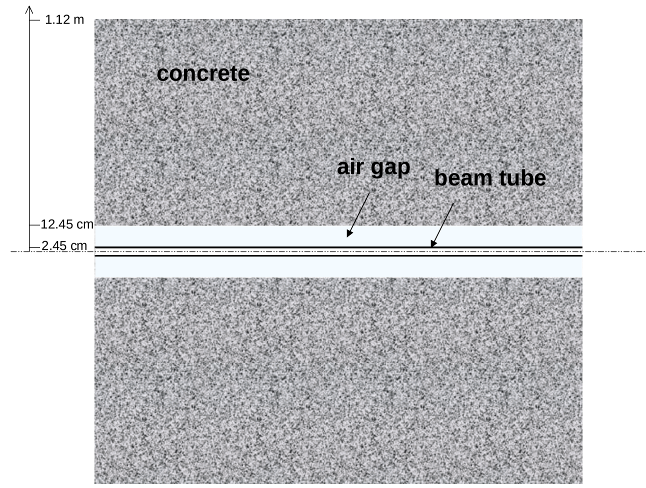

Figure 3: The components of a 1 m long straight section of the beam line with the shielding.

magnet. Since this part of the beam line is not yet designed, we concentrate here on the study of the shielding in the straight section of the beam line.

In Fig. 3 the essential components of the straight section of the beam line are shown. The beam pipe is made of aluminum or stainless steel, and has a thickness around 0.5 cm. Its inner radius must be bigger than 1.3 cm, which will be the radius of the proton beam. After a gap which will have to be big enough to accomodate the focusing quadrupoles, the concrete, in type and amount to be determined, is placed for shielding.

We have studied different shielding options by comparing the results using concrete with and without boron and barium. The effect of the variation of the thickness of the shielding on the effective dose has been determined. More complex shielding combinations have also been considered. The effect of the material and thickness of the beam line on the escaping neutron flux has also been investigated.

2.2.1 Variation of the shielding thickness and composition

In the calculations we used the ordinary concrete and the barytes concrete, as well as ordinary concrete with addition of boron to absorb thermal neutrons. The density of the normal concrete and of the normal concrete with boron is 2.35 g/cm^3, while the density of the barytes concrete is 3.54 g/cm^3. The chemical compositions of the different concretes are given in Fig. 4.

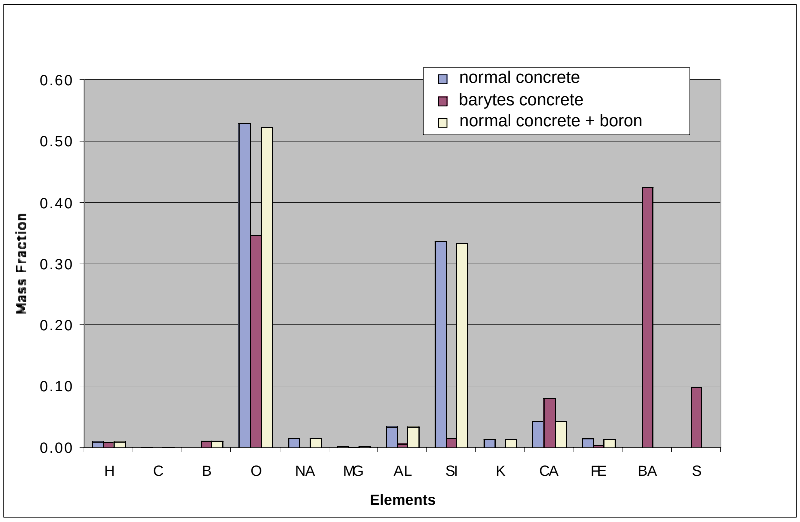

Figure 4: Chemical composition of the three different concrete materials used (in weight fraction).

1) The first study was done on the concrete thickness, varying the thickness of barytes concrete using 1 m, 1.4 m and 2 m radius. The neutron flux escaping the shielding in the three configurations is given in Fig. 5. Increasing the thickness of the shielding by 40-50 cm gives a reduction in the flux, uniform at all the energies, by a factor 10. In Table 1 the integral fluxes of escaping neutron above and below 20 MeV of energy are given. We also indicate the total neutron yield (the number of neutrons produced per primary proton), and the yields in the beam pipe and in the concrete. The yield in the concrete does not increase with the concrete thickness, indicating that practically all the source neutrons are produced within the first meter of shielding.

The particle fluxes obtained using FLUKA and EA-MC were consistent. The effective doses were calculated with FLUKA using Pelliccioni conversion coefficients [6]. In Fig. 6 the spatial distribution of the effective dose for 1 mA of beam loss with a shielding of 1 m of barytes concrete is represented. Assuming beam losses of 10 nA (i.e. 1 nA/m $\times$ 10 m) we obtain in this case the corresponding dose rate of 100 μSv/h, which is 10 times the allowable dose rate in the reactor building for unlimited exposure of personnel. The dose is essentially due to neutrons (90 %

Table 1: Main neutronic parameters versus shielding thickness for barytes concrete and an aluminum beam pipe (0.8 cm thick) per 10 nA of beam losses.

Concrete thickness (m)	Flux of escaping neutrons ($n/cm^2/s$) < 20 MeV	Flux of escaping neutrons ($n/cm^2/s$) > 20 MeV	Total neutron yield	<20 MeV neutron yield	yield in beam pipe	yield in concrete shield
1.0	38	18	0.202	0.167	0.035	0.132
1.4	4	2	0.201	0.167	0.032	0.135
2.0	0.2	0.1	0.203	0.169	0.033	0.136

of the total). Therefore, it is necessary to have a thickness of concrete of at least 1.4 m.

2) The next test was performed by considering different types of concrete. Fig. 7 shows the neutron fluxes in the concrete shield in the three cases. As shown, the presence of boron eliminates the thermal peak and reduces the flux of epithermal neutrons. The spectra in the case of barytes concrete and concrete with boron are similar. However, for the barytes concrete the flux below about 3 MeV is higher, while there are less high-energy neutrons. Clearly, in this case the higher density of the barytes concrete plays a role in slowing down more high-energy neutrons. The increased flux below 3 MeV is due to the (n, Xn) reactions in barium and to the higher spallation neutron yield.

Consequently, the flux of escaping neutrons above and below 20 MeV depends strongly on the type of concrete. The values of the integral flux for escaping neutrons above and below 20 MeV are given in Table 2. The flux with the barytes concrete shielding is roughly a factor 4 lower than the flux with the normal concrete.

This result is achieved despite a neutron yield about 40% higher in the case of the barytes concrete. This effect was investigated by looking at the spectra of the spallation neutrons in the concrete. Fig. 8 shows the source neutrons in concrete below 20 MeV, as well as the source neutrons above 20 MeV, which have been transported below this threshold energy. A few source neutrons are generated above 20 MeV and escape the system. It is clear from the figure that in the case of normal concrete or normal concrete plus boron, the spallation spectrum is composed of one high-energy peak. In the case of barytes concrete, an additional peak centered at about 1.5 MeV is present. Thus, the additional source neutrons,

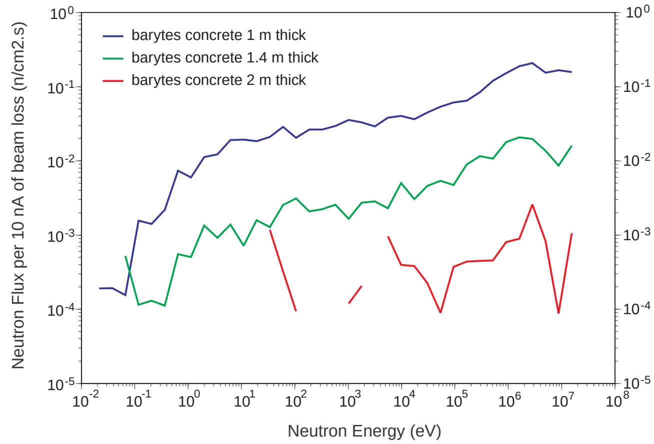

Figure 5: Variation of the neutron flux spectra escaping the beam transfer line as a function of the thickness of the concrete shield.

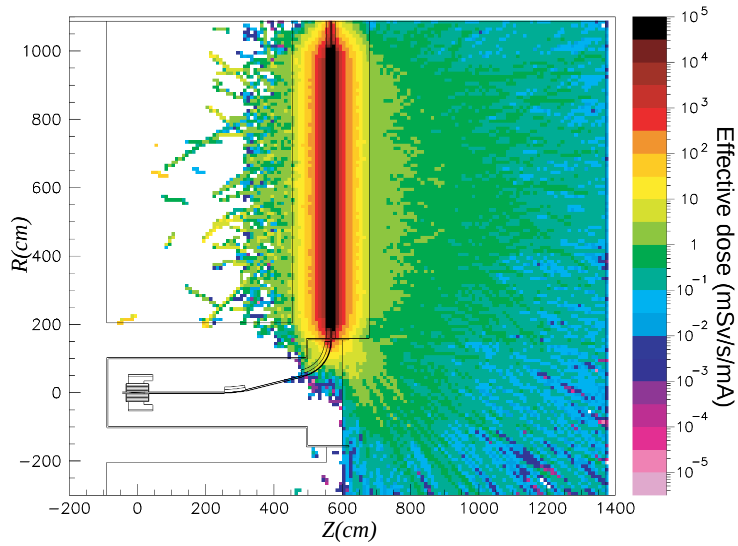

Figure 6: Estimation of the particle dose rate to human body escaping the beam transfer line per mA of beam losses, in the shielding configuration with 1 m thick barytes concrete.

Table 2: Main neutronic parameters versus concrete composition (1.4 m thickness) and an aluminum beam pipe (0.8 cm thick) per 10 nA of beam losses.

Concrete	Flux of escaping neutrons ($n/cm^2/s$) <20 MeV	Flux of escaping neutrons ($n/cm^2/s$) >20 MeV	Total neutron yield	<20 MeV neutron yield	yield in beam pipe	yield in concrete
normal	17	6	0.127	0.095	0.033	0.062
normal+B	7	5	0.127	0.094	0.032	0.062
barytes	4	2	0.201	0.167	0.032	0.135

introduced by using the barytes concrete, have on average a lower energy, so that they are easily moderated and absorbed by the shielding; the presence of barium helps in absorbing also a good fraction of the higher energy neutrons.

As shown below, the decrease of the dose rate is the same as for the flux, making the barytes concret the most effective shielding for the reduction in the dose rate.

3) We considered different shielding options other than having a shielding made only of concrete. In particular, we considered the possibility of having an inner layer of a dense material like copper or iron, followed by barytes concrete. Iron and copper have high density and relatively low-Z, therefore they are excellent materials for rapidly slowing down fast neutrons, which then can be captured by the concrete.

Another option consisted of a buffer of borated polyethylene and a combination of iron and polyethylene. Having pure polyethylene should help in quickly moderate the neutrons.

The integral fluxes and the yields are reported in Table 3. We used a thickness of the Fe/Cu layer of 20 cm. It is clear that the shielding with a 20 cm layer of Fe or Cu results in a further reduction of the flux of escaping neutrons, with respect to the case with only barytes concrete. In fact, as shown in Fig. 9, the effect of the iron layer is to decrease the fraction of fast neutrons coming from the beam tube. The Fe/Cu layer has also the property that the spallation neutrons produced have on average a lower energy and are produced in the inner part of the beam line shielding, thus having a higher probability of being absorbed by the shielding. The overall improvement in the flux with respect to the barytes concrete shielding is of about a factor 4. However, this improvement goes at the expense of an increased weigth and activation of the shielding. It should therefore be used only if absolutely

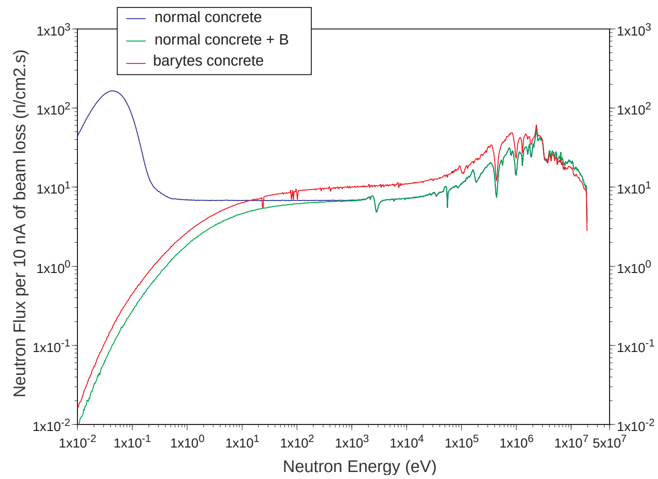

Figure 7: Neutron flux spectra for different compositions of the concrete shielding (1.4 m thick) per 10 nA of beam loss.

Table 3: Main neutronic parameters for different shielding configurations (20 cm of the material indicated in the first column, plus 1.2 m thick barytes concrete) per 10 nA of beam losses.

Inner layer	Flux of escaping neutrons ($n/cm^2/s$) <20 MeV	Flux of escaping neutrons ($n/cm^2/s$) >20 MeV	Total neutron yield	<20 MeV neutron yield	yield beam pipe	yield inner layer	yield concrete
20 cm Cu	1.0	0.5	0.230	0.195	0.105	0.085	0.005
20 cm Fe	1.0	0.6	0.219	0.184	0.104	0.073	0.007
20 cm bor. poly	4.9	1.2	0.166	0.142	0.100	0.015	0.027
5 cm Cu +15 cm bor. poly	3.7	1.7	0.212	0.182	0.101	0.065	0.015

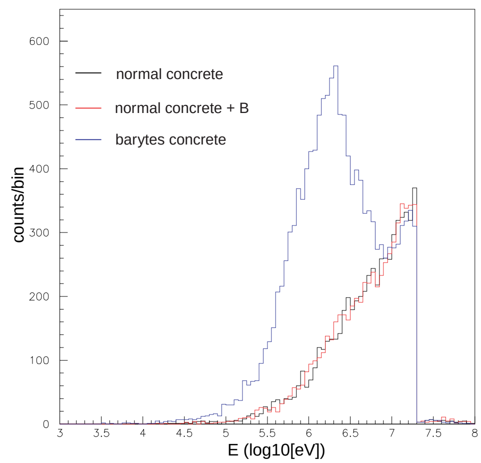

Figure 8: Spallation neutron spectra in the shielding for different concrete compositions. As expected, the spectra are sensitive to the presence of barium. See explanation in the text.

necessary.

In the shielding configurations using polyethylene, there is a decrease in the efficiency of the shielding. This is due to the fact that spallation neutrons in polyethylene have on the average a higher energy, and require more shielding to be stopped.

2.2.2 Variation of the beam pipe material and thickness

The concrete is obviously the most important element in the beam line shielding. However, an additional effect may come from the type and size of the material of the beam pipe. We investigated as possible materials aluminum and stainless steel, using both AISI304 and AISI316.

The test on the material was performed using an 8 mm thick beam pipe, and a barytes concrete shielding 1.4 m thick. With this configuration, an effect is indeed observed in the flux of escaping neutrons, as indicated in Table 4. It is interesting to observe the different features of the spallation neutron spectra with Al and stainless steel beam pipe (Fig. 10). In fact, with an Al beam pipe most of the spallation neutrons are produced in the concrete, while the opposite situation happens with the AISI304 beam pipe. This will have an effect on the neutron flux and on the

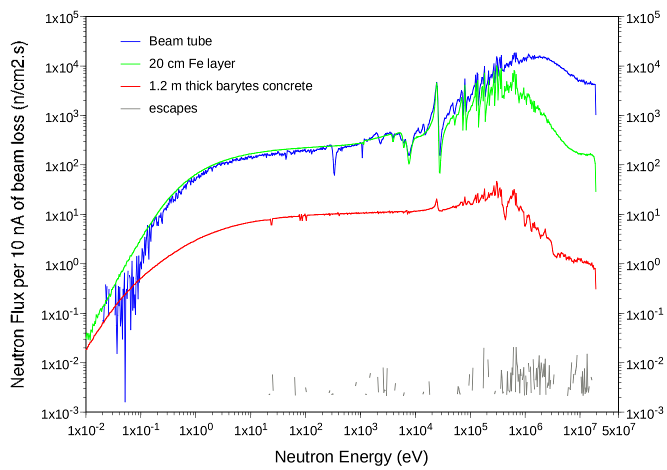

Figure 9: Neutron flux spectra in the different components of the beam transfer line with the shielding option with a Fe layer, per 10 nA of beam loss.

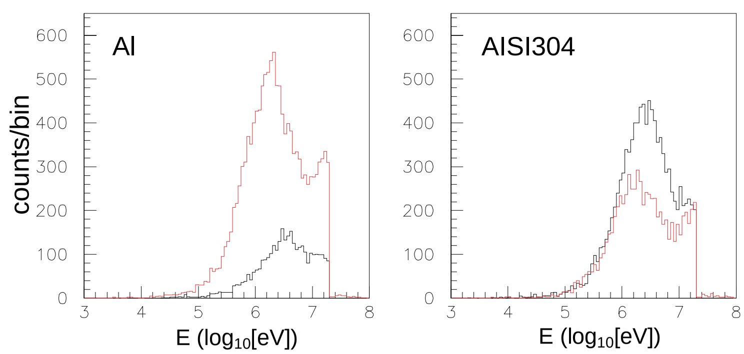

Figure 10: Energy spectra of source neutrons in the beam pipe (black) and concrete (red) with Al and AISI304 beam pipes.

Table 4: Main neutronic parameters versus beam pipe material (of 8 mm thickness) for barytes concrete (1.4 m thick) per 10 nA of beam losses.

Beam pipe material	Flux of escaping neutrons ($n/cm^2/s$) <20 MeV	Flux of escaping neutrons ($n/cm^2/s$) >20 MeV	Total neutron yield	<20 MeV neutron yield	yield in beam pipe	yield in concrete shield
Al	3.6	1.9	0.201	0.167	0.032	0.135
AISI304	3.2	1.3	0.203	0.172	0.104	0.073
AISI316	3.8	1.1	0.208	0.176	0.106	0.070

effective dose. However, this effect will be reduced if a thinner beam pipe is chosen. In fact, there is also an effect on the beam pipe thickness, and a thinner beam pipe is preferable, even though the effect is at the level of 10-20%.

2.2.3 Effective doses

The results from the dose calculations using FLUKA for the different shielding configurations are summarized in Table 5. We neglected the contribution from activation in the calculations.

The shielding around the beam line must comply with the requirement that the personnel be allowed inside the reactor building and in the control room also during the accelerator running phases. These workers will be classified according to italian legislation as "exposed workers of category A", for which the reference annual dose limit is 20 mSv/y. In the control room (at about 7 m from the center of the beam line) exposed workers will be allowed for a complete working shift (2000 h/y) and a design limit 10 times lower than the reference one is assumed in this case as suggested by the italian regulatory authority.

The dose rate at 6-7 m from the beam line must therefore not exceed 1 μSv/h. This means that in contact with the surface, at about 2 m from the proton beam, a dose rate of about 10 μSv/h is acceptable.

Another constraint to the dose rate is due to non-exposed workers walking outside of the reactor building at a minimum distance from the beam of about 20 m. An occupational factor of 1/6 is assumed in this case, and therefore 0.8 μSv/h is the design limit at 20 m distance, which is respected if the conditions for the exposed workers are respected.

Table 5: Effective dose on the surface of the shielding and at 5 m from the same surface, for a beam loss of 1 nA/m along the 10 m of the beam line (straight section), for the different shielding configurations analyzed. The configurations are separated in three groups, having a total shielding thickness of 1 m, 1.4 m and 2 m, respectively. In bold the configuration chosen as reference is indicated.

Beam pipe	Shielding configuration	Effective dose at surface (μSv/h)	Effective dose 5 m from surface (μSv/h)
8 mm Al	1 m normal concrete	350	64
8 mm Al	1 m barytes concrete	100	18
8 mm Al	1.4 m barytes concrete	9.5	2.4
8 mm AISI304	1.4 m barytes concrete	7.9	1.8
2 mm Al	1.4 m barytes concrete	8.3	1.9
2 mm AISI304	**1.4 m barytes concrete**	**7.5**	**1.7**
8 mm AISI304	20 cm Fe, 1.2 m barytes concrete	3.7	0.8
8 mm AISI304	20 cm Cu, 1.2 m barytes concrete	3.2	0.8
2 mm Al	20 cm Cu, 1.2 m barytes concrete	3.9	0.9
2 mm Al	5 cm Cu, 15 cm borated poly 1.2 m barytes concrete	10.5	2.4
2 mm Al	20 cm borated poly 1.2 m barytes concrete	10.8	2.5
2 mm AISI304	2 m barytes concrete	0.4	0.12
8 mm AISI304	20 cm Fe, 1.8 m barytes concrete	0.2	0.06
8 mm AISI304	20 cm Cu, 1.8 m barytes concrete	0.2	0.06

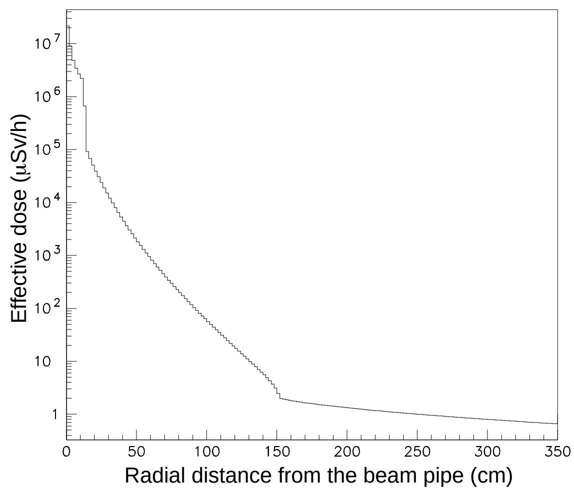

Figure 11: Effective dose as a function of the radial distance to the beam pipe for a beam current of 0.25 mA and 10^{-6}/m beam losses for the reference shielding configuration.

This analysis has shown that it is possible to reduce the effective dose rate due to beam losses in normal operating conditions below the above mentioned limit of 10 μSv/h. This reduction is achieved primarily by increasing the thickness of the concrete shielding. For instance, increasing the thickness by 1 m reduces the dose rate by more than two orders of magnitude. The presence of boron and barium in the concrete is also very important, giving a reduction of the dose rate by nearly a factor 4.

Inserting different Cu or Fe layers can further improve the dose rates emitted at the surface of the concrete shielding. For instance, with a 20 cm thick copper or iron layer surrounded by 1.8 m of barytes concrete, the effective dose at the surface is about 0.2 μSv/h. However, the improvement in the effective dose is achieved at the expense of an increase of activation, as well as in the overall weight of the beam line shielding.

Further reduction of the dose rate can be obtained by changing the composition and thickness of the beam tube. We find that the lowest dose rate is reached by using a thin beam tube made of AISI304.

Given these considerations, the layout consisting of 1.4 m of barytes concrete, with a 2 mm thick AISI304 beam pipe can be adopted as a reference configuration, resulting in an effective dose at the surface of the shielding of 7.5 μSv/h for 1 nA/m beam losses at 1 mA proton current. However, the maximum beam current envisaged during the TRADE experiment will be about 0.25 mA in order not to exceed the limit of 50 kW of beam power imposed by the thermal hydraulic requirements of the spallation target. Consequently, an additional factor 4 should be applied to the doses reported in Table 5, resulting in a effective dose at the surface of about 2 μSv/h for the reference case.

Figure 11 represents the effective dose as a function of the radial distance from the beam pipe for a beam current of 0.25 mA and 10^{-5} beam losses (0.25 nA/m of beam losses along 10 m of beam line) for the reference configuration.

In conclusion, the effective dose obtained for the reference configuration satisfies the safety requirements (at least for the straight section). Moreover, one should also consider that the calculational scheme adopted is a pessimistic one since we have used a user defined source routine which generates protons distributed along the length of the beam pipe and propagated outwards. In reality, the protons exiting the beam line will have a very small angle, and therefore will be attenuated even more. Indeed, we have checked that the reduction factor, assuming a divergence of 1° is of 2.5, reducing the effective dose at the surface of the shielding to about 0.8 μSv/h.

Different considerations should be made for the shielding around the M4 magnet. The design of the shielding around the magnet will have to face the fact that the beam losses in the magnet are two orders of magnitude higher than in the straight section. On the other hand, the loss will be localized in a relatively small spot, making it a point source of neutrons, as opposed to the extended source given by the straight section, which will constitute an advantage since the flux will be decreasing like $1/R^2$ instead of $1/R$.

2.3 Activation

The study of the activation of the different elements of the TRADE experiment is very important because of the presence of the accelerator and the spallation source. One should consider the activation induced by the beam-target interaction, the activation of the water due to beam losses and to neutrons streaming from the reactor core, the air activation and the activation of the beam line due to beam losses in normal conditions. Burnup calculation using the EA-MC code were carried out to study these cases.

1) In the case of the beam-target interactions, we estimated the activation of the tungsten spallation target and its aluminum supports. Burnup calculations were performed up to 1000 years from the experiment. The results are represented in Fig. 12. The activity of the spallation target (expressed in Ci/mA/yr) is dominated by activation resulting from successive thermal neutron captures. After one year of cooling down the activity is dominated by the decay of the spallation products,

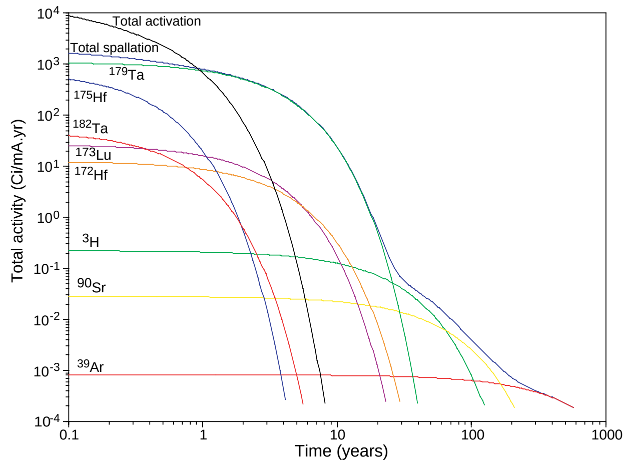

Figure 12: Evolution of the radioactivity (Ci/mA·yr) of the tungsten spallation target as a function of time.

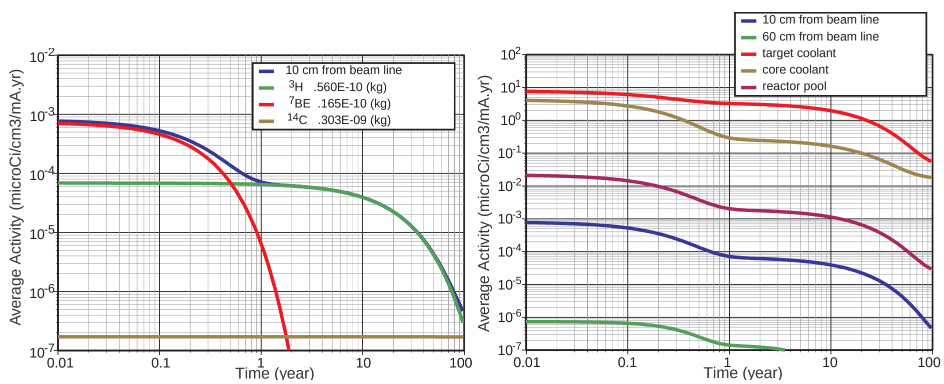

Figure 13: *Left*: Evolution of the radioactivity of water 10 cm from the beam line due to normal beam losses (1 nA/m of beam losses along 6 m of straight section). *Right*: Evolution of the radioactivity of water coolant in different parts of the reactor core.

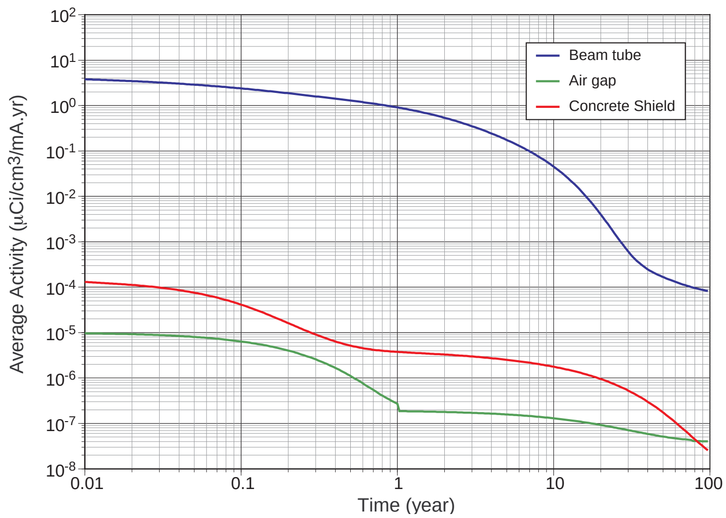

Figure 14: Evaluation of the radioactivity from the beam line due to normal beam losses (1 nA/m of beam losses along 10 m of straigth section.)

mostly Ta, Lu and Hf isotopes. At longer times (> 40 years) tritium and ^{90}Sr are the only isotopes of importance. Tritium is the only volatile isotope produced in the spallation target, which will however be continuously carried away by the vacuum system of the beam pipe.

These activation levels are comparable with those of the fuel elements. Therefore, the safety procedures for the fuel rods will also apply for the spallation target.

2) The activation of water contained around the beam tube during normal operation was also estimated (Fig. 13). The activity of the water 10 cm from the beam line (expressed in μCi/cm^3/mA/yr) is dominated by the decay of the spallation products, mostly ^{7}Be (8×10^{-4} μCi/cm^3/mA/yr). After one year tritium and ^{14}C are the only isotopes of importance. Similarly, the activity of the water surrounding the spallation target and that of core is entirely dominated by beryllium. The level of radioactivity is about 10^4 the one induced in the water around the beam line. Air activation calculations were also performed, as well as ^{16}N production from ^{16}O(n,p)^{16}N, indicating a negligible level of production [2]. These radioactivity levels are very low and do not constitute an issue.

3) Finally, we calculated the activity of the beam transfer line induced by the proton beam losses during normal operation. For these calculations we used a stainless

steel tube, which activates more than aluminum. The activity, shown in Fig. 14, is mostly dominated by the spallation products generated in the beam tube. Again, the level of activation is very low.

3 CONCLUSIONS

This paper concentrated on the radiation protection aspects related to the beam losses in normal operating conditions. A shielding of barytes concrete of 1.4 m thickness is recommended to lower the dose rate below the acceptable limits for the exposed workers. The problem of the losses near the M4 magnet will have to be addressed next.

Another important aspect is beam-target interactions; in this case we have shown that there will be no additional radiation safety issues with respect to the situation related to a normal TRIGA reactor. The only new aspect consists in a slight irradiation of the lower bending magnet.

Calculations show that activation of water, air and beam line will be negligible with respect to the one of the core and of the spallation target. For the spallation target, the same safety procedures for the core elements will have to be applied.

References

[1] The European Technical Working Group on ADS, *A European Roadmap for Developing Accelerator Driven System (ADS) for Nuclear Waste Incineration*, April 2001.

[2] The Working Group on TRADE: TRiga Accelerator Driven Experiment, *TRADE Final Feasibility Report*, March 2002.

[3] A. Herrera-Martínez *et al.*, *Neutronic and Radio-Protection Analysis of the TRiga Accelerator-Driven Experiment (TRADE)*, CERN internal note SL/2002-007, and Proceedings of the 12th Biennial RPSD Topical Meeting, Santa Fe, USA, April 14-18 2002.

[4] A. Fassò, A. Ferrari, P.R. Sala, *Electron - photon transport in FLUKA status*, Proceedings of the Monte Carlo 2000 Conference, Lisbon, October 23-26 2000, A. Kling, F. Barão, M. Nakagawa, L. Távora, P. Vaz eds., Springer-Verlag Berlin, p. 59 - 164 (2001).
A. Fassò, A. Ferrari, J. Ranft, P.R. Sala, *FLUKA: Status and Prospective for Hadronic Applications*, Proceedings of the Monte Carlo 2000 Conference, Lisbon, October 23-26 2000, A. Kling, F. Barão, M. Nakagawa, L. Távora, P. Vaz eds., Springer-Verlag Berlin, p. 955-960 (2001).

[5] Y. Kadi *et al.*, *The EA-MC code package*, in Proceedings of the Fifth International Meeting on Simulating Accelerator Radiation Environment - SARE 5: Models and Codes for spallation neutron sources; OECD Headquarters, Paris, France, July 17-18, 2000.

[6] A. Ferrari and M. Pelliccioni, *Dose equivalents for mono-energetic electrons incident on the ICRU sphere*, Radiation Protection Dosimetry, 55 n. 3, 207-210 (1994) (also LNF-94/005 (P) (1994)).
Dose equivalents for mono-energetic positrons incident on the ICRU sphere, Radiation Protection Dosimetry, 55 n. 4, 309-312 (1994).
Fluence to dose equivalent conversion data and effective quality factors for high energy neutrons, Radiation Protection Dosimetry 76, n. 4, 215-224 (1998).
A. Ferrari, M. Pelliccioni, and M. Pillon, *Fluence to effective dose and effective dose equivalent conversion coefficients for photons from 50 keV to 10 GeV*, Radiation Protection Dosimetry 67, n. 4, 245-251 (1996).
Fluence to effective dose and effective dose equivalent conversion coefficients for electrons from 5 MeV to 10 GeV, Radiation Protection Dosimetry 69, n. 2, 97-104 (1997).
Fluence to effective dose conversion coefficients for protons from 5 MeV to 10 TeV, Radiation Protection Dosimetry 71, n. 2, 85-91 (1997).